Food Chemistry: X 31 (2025) 103196

Contents lists available at ScienceDirect

Food Chemistry: X

journal homepage: www.sciencedirect.com/journal/food-chemistry-x

Stable isotope and multi-elemental analysis combined with statistical modeling for saffron origin authentication

Cathrine Terro [a,b], Lidija Strojnik [b], Doris Potočnik [b], Marta Jagodic Hudobivnik [b], Darja Mazej [b], Luana Bontempo [c], Mahmoud Eddabdouby [d], Nour Eddine Amenzou [d], Benmansour Moncef [d], Simon Kelly [e], Nives Ogrinc [a,b,*]

[a] Jožef Stefan International Postgraduate School, Ljubljana, Slovenia
[b] Department of Environmental Sciences, Jožef Stefan Institute, Ljubljana, Slovenia
[c] Fondazione Edmund Mach, Via E. Mach, 1, 38098 San Michele all'Adige, Italy
[d] Centre national de l'énergie, des sciences et des techniques nucléaires (CNESTEN), Rabat, Morocco
[e] International Atomic Energy Agency (IAEA), Austria

ARTICLE INFO

Keywords:
Saffron
Stable isotope ratio analysis
Elemental analysis
Statistical modeling
Authentication
Traceability
Geographical origin

ABSTRACT

Saffron (*Crocus sativus* L.) is among the world's most valuable spices, yet its high market price and complex supply chains make it particularly vulnerable to mislabeling and fraud. To address this, we integrated stable isotope ratio analysis (δ^2H, δ^{13}C, δ^{15}N, δ^{18}O, δ^{34}S) with multi-elemental profiling and advanced statistical modeling to authenticate saffron geographical origin. A total of 75 saffron samples—48 authentic—sourced from Morocco, Greece, Slovenia, Spain, Iran, and the United Kingdom were analyzed using isotope ratio mass spectrometry (IRMS) and inductively coupled plasma mass spectrometry (ICP-MS). These were combined with two previously published datasets, including 163 authentic samples in total. The incorporation of external datasets was possible due to their strong methodological and analytical comparability with the present study, ensuring directly compatible results. Orthogonal partial least squares discriminant analysis (OPLS-DA) achieved 94 % classification accuracy, identifying δ^2H, δ^{15}N, K, Ca, δ^{13}C, Sr, Mn, Co, and Zn as key variables for discriminating geographical origins. Incorporation of elemental ratios (Rb/Sr, K/Rb, Ca/Sr) and/or δ^{18}O and δ^{34}S further refined classification, particularly improving accuracy for Moroccan saffron. Class-modeling via Data-Driven Soft Independent Modeling of Class Analogy (DD-SIMCA) confirmed high sensitivity and specificity across target sets and revealed potential mislabeling in ~15 % of commercial samples, with the highest discrepancy (24 %) observed in Iranian-labeled products. These findings underscore the power of combined stable isotope and multi-elemental approaches for saffron origin authentication and highlight the need for robust analytical verification to strengthen transparency and combat fraud in the saffron trade.

1. Introduction

Saffron, derived from the dried stigmas of *Crocus sativus*, is one of the most valuable and sought-after spices in the world. Known as "red gold," it is prized for its vibrant color, unique aroma, and versatility in culinary, medicinal, and industrial applications, including textiles, dyes, and pharmaceuticals. Its production dates back to ancient civilizations, including the Egyptians, Greeks, and Romans, underscoring its enduring cultural and economic importance (Mousavi & Bathaie, 2011; Mzabri et al., 2019). Over the centuries, its cultivation has flourished in regions such as Iran, India (Kashmir), Greece, and Spain, which are renowned for producing some of the world's finest saffron (Gresta et al., 2009; Mousavi & Bathaie, 2011). Iran, in particular, remains the largest global producer, supplying approximately 80 % of the world's saffron (Menia et al., 2018). Saffron's economic and cultural significance is deeply tied to its geographic origin, which impacts quality, consumer trust, and market value.

The production of saffron remains highly labor-intensive, requiring nearly 400 h to yield just 0.5 g of dried stigmas from 75 to 100 flowers (Cardone et al., 2019). This intensive hand cultivation contributes to its scarcity and high market value. Its unparalleled aesthetic and organoleptic qualities are attributed to bioactive compounds such as crocin,

* Corresponding author at: Jožef Stefan International Postgraduate School, Ljubljana, Slovenia.
E-mail address: nives.ogrinc@ijs.si (N. Ogrinc).

https://doi.org/10.1016/j.fochx.2025.103196
Received 23 March 2025; Received in revised form 1 October 2025; Accepted 20 October 2025
Available online 22 October 2025

safranal, and picrocrocin, which contribute to its distinct flavour and health benefits, including antioxidant, anticancer, and anti-inflammatory effects (Shahi et al., 2016; Moradi Rikabad et al., 2019; Mykhailenko et al., 2020).

Local conditions contribute to the distinctive chemical profiles of saffron, which are often considered key markers of quality (Gresta et al., 2009; Mousavi & Bathaie, 2011; Mykhailenko et al., 2020). Optimal cultivation occurs in loose, well-irrigated, and effectively drained clayey-calcareous soils, further emphasizing the importance of geographic and environmental suitability (Zarghani et al., 2016). Changes in temperature, precipitation, and other climatic variables can significantly impact production, as evidenced by studies in the Kashmir Valley showing that rising temperatures and altered precipitation patterns have led to a decline in saffron yields over recent decades (Ayoub et al., 2024). Beyond climate, factors such as altitude, soil composition, water availability, photoperiod, and fertilization practices are equally critical for influencing saffron's growth and chemical composition (Cardone et al., 2020; Rahimi et al., 2017; Siracusa et al., 2010). Although its sensitivity to environmental conditions has limited its cultivation (Cardone et al., 2019), saffron production has expanded to other countries, including Italy, Turkey, France, Switzerland, Pakistan, China, Japan, and Australia. This global expansion reflects both the rising demand for saffron and the ability of cultivation practices to adapt to diverse climates and environments.

Saffron's high economic value also makes it vulnerable to various types of fraud, including mislabeling, dilution, and substitution. As global trade grows, fraudulent practices threaten the reputation of authentic producers and devalue traditional saffron-growing regions, making reliable geographic origin verification essential for ensuring authenticity, protecting market value, and preserving the cultural and economic heritage of these areas (Gresta et al., 2009). Techniques like genetic markers, sensory analysis, and chemical profiling are commonly used to authenticate saffron, each providing distinct insights. For example, dilution, where pure saffron is mixed with other substances such as paprika or turmeric (botanical adulterants), can be detected through chromatographic and spectroscopic methods that analyze the chemical composition and purity of the product (Ryparova Kvirencova et al., 2023). Substitution, involving the sale of different materials like turmeric, safflower, paprika, or marigold flowers, can be uncovered using DNA-based methods and chemical fingerprinting (Bhooma et al., 2023). The enhancement of saffron's color using synthetic dyes such as Sudan I-IV and Rhodamine B, which are potentially genotoxic, can also be detected through high-performance liquid chromatography (HPLC) and mass spectrometry (Bhooma et al., 2020; Koocheki & Milani, 2020).

Mislabeling, where the origin of saffron is falsely claimed, can be identified using stable isotopic and multi-elemental analysis, which relies on the sophisticated and widely used stable isotope approach by examining the isotopic composition of the light elements $^{2}H/^{1}H$, $^{13}C/^{12}C$, $^{15}N/^{14}N$, $^{18}O/^{16}O$, and $^{34}S/^{32}S$ (Salehi et al., 2022). By analyzing these isotopic ratios, unique geographical and environmental fingerprints for each product can be created due to factors that can affect their isotopic abundance through fractionation, such as origin, climatic conditions, soil properties, and the geology of the regions where food ingredients are grown (Kelly et al., 2005).

When combined with elemental analysis, verification becomes even more powerful. The availability of elements depends on various factors, including soil pH, moisture, clay and other characteristics (Katerinopoulou et al., 2020), such as water availability and climate, while elements such as Sr, Ba, Cs, S, Mo, and Ni are related to geology (Saaltink et al., 2014). Strontium is already widely used to trace the geographical origin of agricultural produce (Hiraoka et al., 2016). Equally, Rb and Cs can be quickly mobilized in the soil and taken up by plants, making them suitable source markers (Kelly et al., 2005). The content of Na is also related to the distance to the sea, and elevated amounts can be found within several kilometres of the coast due to the steady input of marine aerosols (Saaltink et al., 2014).

Phosphorus levels in food products are often influenced by the application of phosphoric fertilizers and agrochemicals. While earlier work (Smith, 2005) suggested that fertilization has a negligible effect on elemental composition relevant to origin prediction, more recent studies challenge this assumption. For instance, a traceability study on highland barley (*Hordeum vulgare* L.) grown in Tibet demonstrated that fertilizer treatments (urea and diamine phosphate) significantly affected the concentrations of key mineral elements, including phosphorus (P), potassium (K), iron (Fe), and copper (Cu), which contributed to improved geographic classification accuracy (Zhao et al., 2022). Furthermore, elevated concentrations of certain elements such as arsenic (As), cadmium (Cd), and copper (Cu) may also result from the intensive use of fertilizers and pesticides, particularly in regions with intensive agricultural practices (Skordas et al., 2013). This highlights the importance of critically evaluating which elements are suitable for use as geographic markers, as some may reflect anthropogenic inputs rather than environmental or geological signatures.

The combination of stable isotope and elemental analysis has been successfully applied to a variety of high-value food products, such as honey (Bontempo et al., 2017; Wu et al., 2015), olive oil (Camin et al., 2010), paprika and cinnamon (Brunner et al., 2010; Primožič et al., 2025), apple juice (Bizjak Bat et al., 2016), strawberries (Strojnik et al., 2022), seafood and shellfish (Luo et al., 2019; Ni et al., 2022), beef (Bai et al., 2025), and lamb (Liu et al., 2021). In addition, it has been applied to rice, garlic, and Chinese medicinal materials (Giannioti et al., 2024; Opatić et al., 2017; Zhang et al., 2022).

Despite their proven utility, limited research has been conducted on the application of these analytical methods for authenticating the geographical origin of saffron (Maggi et al., 2011; D'Archivio et al., 2014; D'Archivio et al., 2019; Rocchi et al., 2019; Wakefield et al., 2019; Perini et al., 2020; Ghiasi & Parastar, 2021; Ibourki et al., 2022; Moras et al., 2022; Nie et al., 2023). Most focus on either elemental analysis or isotopic analysis, rarely integrating both. Notable exceptions include Perini et al. (2020) and Wakefield et al. (2019). Furthermore, studies do not fully utilize all five isotopic ratios ($\delta^{2}H$, $\delta^{13}C$, $\delta^{15}N$, $\delta^{18}O$, and $\delta^{34}S$), which are essential for capturing the complexity of saffron's chemical and isotopic profiles. Studies also tend to focus on one or two countries, with Morocco, a major saffron producer, frequently underrepresented in favor of Iran, Greece, Spain, and Italy.

This study analyzes authentic saffron samples from producers in Iran, Greece, the United Kingdom, Slovenia, Spain, and Morocco, with a particularly strong representation of Moroccan saffron. It also analyzes commercial samples from Iran, Greece, Spain, Italy, India, and Afghanistan, as well as integrating data from Perini et al. (2020) and Wakefield et al. (2019). Using this expanded dataset, advanced statistical techniques, including Data-Driven Soft Independent Modeling of Class Analogies (DD-SIMCA), were applied to verify the origin of both commercial and authentic saffron samples. By combining the available datasets, we aim to demonstrate that isotopic and elemental data are sufficiently robust and standardized to allow integration across studies, thereby strengthening the statistical power of the analysis and underscoring their potential for broader applications in future research.

2. Materials and methods

2.1. Sample collection

In total, 75 samples were included in this study (Table S1). Samples were collected in three sets: (1) samples collected directly from the producers to provide authentic samples, including from Morocco (n = 41), Greece (n = 3), United Kingdom (n = 1), Slovenia (n = 1), Spain (n = 1), and Iran (n = 1); (2) 25 samples of unverified origin, purchased from local supermarkets in Belgium (n = 3), Slovenia (n = 2), Greece (n = 6), Spain (n = 7), Italy (n = 5), and The Netherlands (n = 2), and (3) commercial saffron samples (n = 2) sourced online. The samples weighed between 0.05 g and 1 g and were either in filaments or powder

form. Dry samples were further homogenized using a ceramic mortar and pestle and stored at room temperature until analysis.

2.2. Data set compilation

Data from Perini et al. (2020) and Wakefield et al. (2019) were also integrated into the database. These datasets were incorporated due to their strong methodological and analytical comparability with the present study, ensuring that the results are directly compatible. Similar to the present study, both used isotope ratio mass spectrometry (IRMS) to analyze the isotopic composition and inductively coupled plasma mass spectrometry (ICP-MS) the elemental composition of saffron from different countries and regions with a focus on distinguishing saffron by production. Additionally, both studies utilized multivariate models—such as PLS-DA, SIMCA, and LDA. Wakefield's study, which was conducted in 2010 and 2011, focused on samples from Iran and Spain, while Perini et al.'s study (2016 to 2019) expanded the geographic coverage by including samples from Italy, Iran, and Morocco.

The present study was conducted in 2023 and includes samples from Morocco, Greece, the United Kingdom, Slovenia, Spain, and Iran. The present study also includes a significant number of Moroccan samples ($n = 41$) collected from villages near Taliouine ($n = 30$) in the Taroudant region, where Perini's samples were sourced. The present study also collected samples from Rif (Zaitoune, $n = 2$) and Sidi Hssain (Do Agadir, Ighri, Timasinine, $n = 9$), which are geographically distant from Taliouine, further expanding the geographic scope.

Together, these three studies contributed a total of 163 authentic saffron samples, including those from Morocco ($n = 53$), Iran ($n = 52$), Italy ($n = 44$), Spain ($n = 9$), Greece ($n = 3$), the United Kingdom ($n = 1$), and Slovenia (n = 1). All samples were obtained directly from producers or certified cooperatives, as also reported by Perini et al. (2020) and Wakefield et al. (2019), ensuring their traceability and authenticity. This combined dataset, excluding commercial samples, forms part of the IsoFoodTrack database (Terro et al., 2025), accessible at http://isofoodtrack.ijs.si/, and will serve as the reference set for the subsequent statistical analyses aimed at evaluating the authenticity and geographic origin of saffron. The distribution of samples is uneven across countries, with the majority originating from Morocco (32.5 %), Iran (31.9 %), and Italy (27.0 %), while the United Kingdom (0.6 %), and Slovenia (0.6 %) are less represented (Fig. 1). Table 1 represents the total number of samples, their origins, the analytical techniques employed, and the isotopes and elements analyzed.

Table 1
Total number of samples, origins, analytical techniques employed, and isotopes and elements analyzed.

Study	Type, number of samples and country of origin	Year	Method	Isotopes	Elements
Wakefield et al., 2019	Authentic: 48 Country: Iran, Spain Commercial: 2 Country: Spain	2010 2011	IRMS ICP-MS	3 isotopes: δ^2H, δ^{13}C, δ^{15}N	42 elements Li, B, Na, Mg, Al, K, Ca, V, Cr, Mn, Fe, Co, Ni, Cu, Zn, As, Se, Rb, Sr, Y, Mo, Ag, Cd, Sn, Sb, Cs, Ba, La, Ce, Pr, Nd, Sm, Eu, Gd, Dy, Ho, Er, Tm, Yb, Lu, Pb, U
Perini et al. 2020	Authentic: 67 Country: Italy Morocco, Iran Commercial: 9 Country: N/A	2016 2017 2018 2019	IRMS ICP-MS	5 isotopes: δ^2H, δ^{13}C, δ^{15}N, δ^{34}S, δ^{18}O	42 elements Li, Be, B, Na, Mg, Al, K, Ca, Sc, Ti, V, Cr, Mn, Fe, Co, Ni, Cu, Zn, Ga, As, Rb, Sr, Y, Zr, Nb, Mo, Ag, Cd, Cs, Ba, La, Ce, Pr, Nd, Sm, Eu, Dy, Ho, Er, Hf, Re, Pb
Our study	Authentic: 48 Country: Morocco, Greece, United Kingdom, Slovenia, Spain, Iran Commercial: 27 Country: Iran, Greece, Spain, Italy, India, Afghanistan	2023	IRMS ICP-MS QQQ	5 isotopes: δ^2H, δ^{13}C, δ^{15}N, δ^{34}S, δ^{18}O	26 elements Na, Al, Mg, P, S, K, Ca, V, Cr, Mn, Fe, Co, Ni, Cu, Zn, As, Se, Rb, Sr, Cd, Mo, Cs, Ba, Hg, and Pb

Fig. 1. Locations of authentic saffron samples (Italy, Morocco, Iran, Spain, Slovenia, United Kingdom, Greece).

2.3. Stable isotope analysis

2.3.1. Determination of $\delta^{13}C$, $\delta^{15}N$, $\delta^{34}S$ values in bulk saffron samples

The stable isotope ratios of carbon ($^{13}C/^{12}C$), nitrogen ($^{15}N/^{14}N$) and sulfur ($^{34}S/^{32}S$) were simultaneously determined in homogenized dry saffron samples using an IRMS equipped with a preparative module for solid samples IsoPrime100 – Vario PYRO Cube (OH/CNS Pyrolyser/ Elemental Analyzer) (IsoPrime, Cheadle, Hulme, UK). Approximately 5 mg of each sample and the same amount of WO_3 were placed in a tin capsule. The capsule was then closed with tweezers and placed in the sampler of the elemental analyzer. The results for carbon, nitrogen and sulfur were normalized against the following international reference materials USGS 88 ($\delta^{13}C = -16.06 \pm 0.07$ ‰, $\delta^{15}N = 14.96 \pm 0.14$ ‰, $\delta^{34}S = 17.10 \pm 0.44$ ‰), USGS89 ($\delta^{13}C = -18.13 \pm 0.07$ ‰, $\delta^{15}N = 6.25 \pm 0.10$ ‰, $\delta^{34}S = 3.86 \pm 0.40$ ‰); USGS91 ($\delta^{13}C = -28.28 \pm 0.08$ ‰, $\delta^{15}N = 1.78 \pm 0.12$ ‰, $\delta^{34}S = -20.85 \pm 0.40$ ‰), USGS43 ($\delta^{15}N = 8.44 \pm 0.10$ ‰, $\delta^{34}S = 10.46 \pm 0.22$ ‰); and IAEA-600 ($\delta^{13}C = -27.77 \pm 0.04$ ‰, $\delta^{15}N = 1.00 \pm 0.20$ ‰). The laboratory reference material CRP-CASEIN with $\delta^{13}C = -20.3 \pm 0.09$ ‰, $\delta^{15}N = 5.62 \pm 0.19$ ‰, $\delta^{34}S = 4.18 \pm 0.74$ ‰) was used for the control. The results were expressed as mean values and were calculated from triplicate analyses. The reproducibility for $\delta^{13}C$ and $\delta^{15}N$ was ±0.2 ‰, and ± 0.7 ‰ for $\delta^{34}S$.

2.3.2. Determination of $\delta^{2}H$ & $\delta^{18}O$ of saffron samples

For determining the $^{2}H/^{1}H$ and $^{18}O/^{16}O$ ratios, about 0.2 mg (between 0.20 and 0.26 mg) of each sample was weighed directly into a silver capsule and simultaneously measured on a DELTA XP IRMS (Thermo Scientific) coupled with TC/EA pyrolyzes (Thermo Finnigan). In order to remove the exchangeable hydrogen effect, the packed reference materials and samples were left open in the laboratory for 5 days in a desiccator to reach an equilibration for exchangeable hydrogen in the organic matrix with environmental hydrogen. Each sample was measured twice, and the mean values were considered. Normalization of results was performed based on two reference materials: CBS (Caribou Hoof Standard) with $\delta^{2}H$ values of −157 ± 0.9 ‰ and $\delta^{18}O$ values of 3.8 ± 0.3 ‰, and KHS (Kudu Horn Standard) with an average $\delta^{2}H$ value of −35.3 ± 1.1 ‰ and $\delta^{18}O$ value of 20.3 ± 0.3 ‰. Measurement precision was ±0.5 ‰ for $\delta^{18}O$ and ± 1 ‰ for $\delta^{2}H$.

All isotopic ratios are reported using the δ – notation in ‰ (Eq. (1)):

$$\delta\left({}^{i/j}E\right) = \delta^{i/j}E = \frac{{}^{i/j}R_P - {}^{i/j}R_{Ref}}{{}^{i/j}R_{Ref}} \quad (1)$$

where superscripts *i* and *j* denote the highest and the lowest atomic mass number of element E, and R_P and R_{Ref} indicate the ratio between the heavier and the lighter isotope ($^{2}H/^{1}H$, $^{13}C/^{12}C$, $^{18}O/^{16}O$, $^{15}N/^{14}N$, $^{34}S/^{32}S$) in the sample (P-product) and reference material (Ref), respectively (Brand et al., 2014). The $\delta^{2}H$ and $\delta^{18}O$ values are reported relative to the V-SMOW (Vienna-Standard Mean Ocean Water) standard, $\delta^{13}C$ values to the V-PDB (Vienna-Pee Dee Belemnite) standard, and the $\delta^{34}S$ sulfur values relative to the V-CDT (Vienna Cañon Diablo Troilite) standard. The $\delta^{15}N$ values are reported relative to AIR.

2.4. Elemental analysis

Approximately 0.15 g of the dry sample was weighed into a Teflon digestion vessel, and 1 mL of Suprapur 65 % HNO_3 (Carlo Erba) was added. The contents were then digested using the Ultrawave digestion system (Single Reaction Chamber Microwave Digestion System, Milestone, Italy). The program was as follows: heating to 240 °C in 20 min, holding for 15 min at max 100 bar at a max power of 1500 W. The digestate was diluted to 10 mL with Milli-Q water (Merck, Millipore, Watertown, MA, USA) and further diluted with 5 % HNO_3 in a ratio 1:5 and 1:10. Selected elements — sodium (Na), aluminum (Al), magnesium (Mg), phosphorus (P), sulfur (S), potassium (K), calcium (Ca), vanadium (V), chromium (Cr), manganese (Mn), iron (Fe), cobalt (Co), nickel (Ni), copper (Cu), zinc (Zn), arsenic (As), selenium (Se), rubidium (Rb), strontium (Sr), cadmium (Cd), molybdenum (Mo), cesium (Cs), barium (Ba), mercury (Hg), and lead (Pb) — were determined using an ICP-QQQ (Agilent 8800, Japan). Quantification was achieved using external calibration. For quality control, every tenth sample was prepared in duplicate, blank and selected reference materials (Spinach Leaves NIST 1570, Tomato Leaves NIST 1573a, Peach Leaves NIST 1547) were also prepared in the same way as the samples. Detection limits were established based on standard deviations of blank measurements, with detailed optimization described in Potočnik et al. (2021). The LoDs are presented in Table S2.

2.5. Statistical evaluation

Preliminary exploratory statistical analysis of the data was conducted using box plots to visualize and compare the distribution of isotopes and elements across different years and countries. The Kruskal-Wallis test, a non-parametric method, was used to identify statistically significant differences ($p < 0.05$) among different saffron samples using the XLSTAT software package (ADDinsoft, New York, USA). For the merged analysis, only elements that met the following criteria were retained: (i) measured in all three datasets, (ii) consistently detected above the limit of detection (LOD) in more than 30 % of total samples, and (iii) demonstrated acceptable data quality suitable for robust statistical modeling. As a result, 18 elements were included in the statistical analysis: macronutrients – magnesium (Mg), potassium (K), calcium (Ca), and sodium (Na); trace elements aluminum (Al), manganese (Mn), iron (Fe), copper (Cu), zinc (Zn), molybdenum (Mo), vanadium (V), and cobalt (Co); earth elements - rubidium (Rb), barium (Ba), strontium (Sr), and cesium (Cs); and potentially toxic elements - cadmium (Cd) and arsenic (As). Each value was then divided by the LOD and taking the natural logarithm of the result, which converts distributions with long "tails" _into a more Gaussian form (Mahynski et al., 2025). We generally found the logarithm to be unnecessary during modeling, though it was initially used to remove outliers from the data.

Orthogonal Partial Least Squares Discriminant Analysis (OPLS-DA) was employed to explore the relationships between predefined categories or groups within the data using SIMCA-P (version 15, Sartorius Stedim Biotech, Umeå, Sweden). The model's predictive performance was evaluated R2X(cum), R2Y(cum) and Q2(cum). Model robustness was confirmed by permutation testing ($N = 100$) and by CV-ANOVA (Fiamegos et al. (2021). Candidates for discriminant markers were selected based on the Variable Importance in Projection (VIP) values from the OPLS-DA models. All VIP values >1 were considered significant and used as the threshold for selecting the most relevant discriminant markers for distinguishing between groups. The Data-Driven Soft Independent Modeling of Class Analogy (DD-SIMCA) method was also applied to validate class membership since class modeling is more suitable than classification methods for controlling the origin or authenticity of foods (Forina et al., 2008). DD-SIMCA analyses were conducted utilizing the modified DD-SIMCA MATLAB GUI tool (Zontov et al., 2017) alongside the mdatools package in R version 4.0.3 (Kucheryavskiy, 2020) described in more detail by Strojnik et al. (2022) and Mahynski et al. (2025). Sensitivity and specificity were used as figures of merit. The sensitivity denotes a share of correctly identified samples of the target class, while specificity is a portion of objects of an alternative class correctly identified as members of that alternative class. The sensitivity can be defined as 100 (1– α)% and specificity as 100 (1– β)% (Fidelis et al., 2017; Rodionova, Oliveri, & Pomerantsev, 2016; Rodionova, Titova, & Pomerantsev, 2016). In addition to sensitivity and specificity, the DD-SIMCA models were also evaluated using total efficiency (TEFF), calculated as: TEFF = (Sens+Spec)/2.

3. Results and discussion

3.1. Exploratory statistical analysis

3.1.1. Temporal variation

Variability between production years must be considered when creating an adequate training set for the model to improve the reliability of geographic origin determination. In this study, a sufficient number of samples from different production years were only available for Morocco, Italy, and Iran. A Kruskal-Wallis test was then applied to determine statistically significant differences ($p < 0.05$) in the variables across sampling years (Table 2; Fig. S1).

The results highlight year-to-year fluctuations in environmental and agricultural conditions influencing the isotopic and elemental profiles of the samples. a broader range from −105.3 ‰ to −69.7 ‰, suggesting greater variability in environmental water sources. Statistically significant temporal patterns have been observed in δ^2H and $\delta^{18}O$ values in Italian saffron illustrating further their sensitivity to climatic conditions. For instance, the Italian saffron samples show an increase in $\delta^{18}O$ values between 2016 and 2017, coinciding with a fourfold reduction in precipitation, particularly in October, just before the harvest (Perini et al., 2020). A positive correlation was observed between δ^2H and $\delta^{18}O$ values ($\delta^2H = 3.44 \cdot \delta^{18}O - 168$ ‰; $r^2 = 0.534$), indicating the influence of biosynthetic fractionation within the plant. The weaker correlation and lower slope compared to the meteoric water line ($\delta^2H = 8 \cdot \delta^{18}O + 10$ ‰) suggest that, while plant tissues retain part of the environmental water signal, deviations arise from physiological processes. The observed correlation between δ^2H and $\delta^{18}O$ suggests that comparable isotopic approaches hold considerable potential for tracing and geolocating the origin of saffron. Further the only statistically significant difference in stable isotope analysis was determined in $\delta^{13}C$ values in Iranian samples, with mean values of −25.1 ‰ in 2016, −24.4 ‰ in 2017, −25.0 ‰ in 2018, and − 26.4 ‰ in 2023, with the more negative value observed in 2023 likely reflecting improved water availability or different climatic conditions, which reduced water stress compared to earlier years.

In Morocco, with the exception of Mg, which showed a decreasing trend over time, other elements such as P, K, Ca, and Cu show statistically significant increasing trend with production year. Other elements like Sr and Zn showed more variability but also revealed significantly higher levels in 2023. This trend can be attributed to Morocco's intensified efforts to improve soil fertility and agricultural productivity. Initiatives such as the Fertimap program, which provides tailored fertilizer recommendations based on detailed soil fertility mapping (Starling, 2023), have likely contributed to elevated levels of these elements in soils (Starling, 2023). Additionally, prolonged drought conditions may have concentrated certain minerals in soils due to reduced leaching, further influencing these observed increases (Toreti et al., 2023). Notably, $\delta^{15}N$ values in Moroccan samples decreased from 8.1 ‰ (SD = 1.02) in 2016 to 5.2 ‰ (SD = 3.71) in 2023, consistent with shifts in agricultural practices and fertilizer use in Morocco.

A similar situation was also observed in Iran, where the concentrations of elements exhibited significant variability between production years. For example, K levels initially increased, peaking before a decline in 2023, while Ca levels showed a notable peak followed by a decrease in 2023. Iron concentrations also varied over the years, while Cu showed a slight increase. Similarly, as in Moroccan saffron, levels of Zn significantly rose during the sampling period while Sr levels fluctuated. Mo and V levels both showed gradual increases, respectively. Cadmium (Cd) and arsenic (As) levels also exhibited variability. Cadmium reached its peak in 2023, while As concentrations fluctuated over the years, initially showing a sharp increase followed by moderate fluctuations in the subsequent years leading up to 2023.

3.1.2. Geographical variation

For the geographical comparison, all available countries were included to capture the broader spatial variability. The isotopic composition of δ^2H, $\delta^{13}C$, $\delta^{15}N$, $\delta^{18}O$, and $\delta^{34}S$ varied across the studied regions and can be visualized in Fig. 2. To contextualize these results, a comparative summary of published stable isotope data for saffron from various geographic origins was compiled (Table S3). This table presents sample origins along with corresponding isotopic ranges, means, and standard deviations, facilitating cross-comparison of isotopic signatures across regions.

Statistically significant differences ($p < 0.05$) were observed for all variables, except for Cu ($p = 0.064$). Differences between countries in variables such as δ^2H, $\delta^{13}C$, Na, Al, and Zn were highly significant ($p < 0.0001$), suggesting their potential utility as discriminant markers for geographical authentication. Notably p-values <0.0001 for δ^2H, $\delta^{13}C$ values and the elemental concentrations of magnesium (Mg), potassium (K), calcium (Ca), sodium (Na), aluminum (Al), manganese (Mn), iron (Fe), zinc (Zn), barium (Ba), strontium (Sr), molybdenum (Mo), vanadium (V), cobalt (Co), cadmium (Cd), arsenic (As), and cesium (Cs). These data are presented in table S4 and visualized in Fig. S2 for Italy, Morocco and Iran.

δ^2H values ranged from −105.3 ‰ (Italy) to −51.0 ‰ (Morocco), with Italian saffron exhibiting the lowest mean δ^2H (−87.8 ‰, SD: 7.2 ‰) and Moroccan samples the highest (−70.7 ‰, SD: 9.0 ‰). Notably, Maggi et al. (2011) reported substantially less negative δ^2H values for Italian saffron (−72.4 ‰), contrasting with those observed in the present study and closer to Moroccan averages. This discrepancy likely reflects regional climatic differences, as Maggi et al.'s samples originated from Sardinia, a Mediterranean island with a warmer, drier climate and isotopically enriched precipitation. In the Medio Campidano saffron-growing area of Sardinia, mean annual temperatures are ~17–18 °C and annual precipitation averages ~450–600 mm, reflecting the region's warm, semi-arid Mediterranean climate (ISPRA, 2020). In contrast, Perini et al. (2020) predominantly included samples from central Italy (L'Aquila and Spoleto), where higher altitude, cooler mean annual temperatures (~10–12.5 °C), and moderate annual precipitation (~ 700–900 mm) contribute to more depleted δ^2H values (−87.8 ‰)

Table 2
Overview of isotope and elemental markers with statistically significant differences in saffron samples from Italy, Morocco, and Iran across different years. Asterisks indicate the level of statistical significance (*p < 0.05; **p < 0.01; ***p < 0.001) for each variable between geographic origins. Blank cells indicate non-significant differences.

Variable	Italy (2016–2017)	Morocco (2016–2018–2019–2023)	Iran (2016–2017–2018-2023)
δ^2H [‰]	*		
$\delta^{18}O$ [‰]	***	***	
$\delta^{34}S$ [‰]			
$\delta^{13}C$ [‰]			*
$\delta^{15}N$ [‰]			
Mg [mg/g]		**	
K [mg/g]		***	**
Ca [mg/g]		**	**
Na [µg/g]			
Al [µg/g]			
Mn [µg/g]			
Fe [µg/g]			*
Cu [µg/g]		**	**
Zn [µg/g]		***	***
Rb [µg/g]			*
Ba [µg/g]			
Sr [µg/g]		*	*
Mo [µg/g]			*
V [ng/g]			*
Co [ng/g]			
Cd [ng/g]			*
As [ng/g]			*
Cs [ng/g]			

Note: *p < 0.05 = statistically significant; ** p < 0.01 = highly significant; ***p < 0.001 = very highly significant.

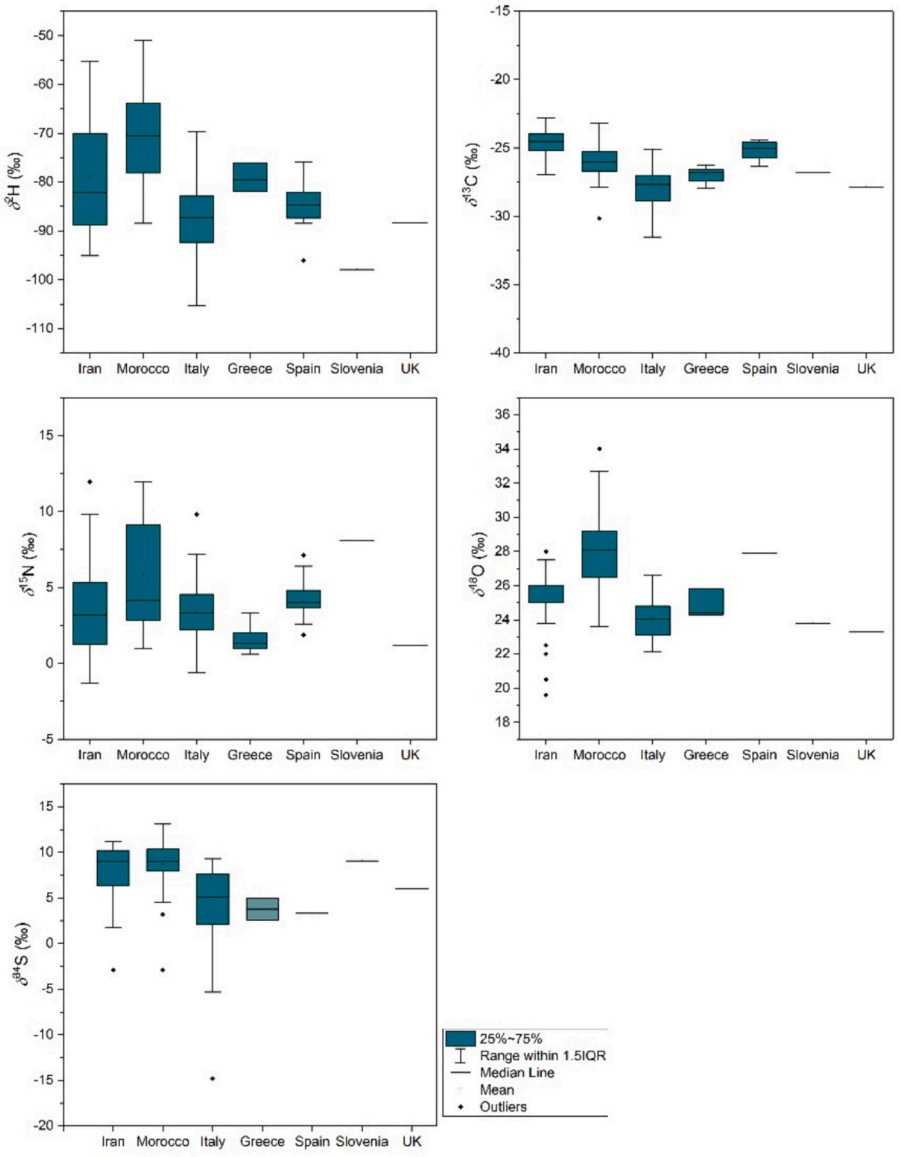

Fig. 2. Box plots of δ^{2}H, δ^{13}C, δ^{15}N, δ^{18}O, δ^{34}S values in saffron samples from Iran, Morocco, Italy, Greece, Spain, Slovenia, and the United Kingdom.

(Climate-Data.org, 2025). These findings underscore the sensitivity of δ^{2}H to local agroclimatic conditions and demonstrate the power of stable isotope analysis in discriminating not only between countries, but also between subregional origins within the same country.

Spain showed the highest δ^{18}O value in our dataset (27.9 ‰), however, this is based on a single sample ($n = 1$) and therefore cannot be interpreted as a population estimate. Thus, Morocco exhibits the highest country-level mean (27.6 ‰, SD: 2.3 ‰), followed by Iran (25.8 ‰, SD: 1.2 ‰), Greece (24.8 ‰, SD: 0.8 ‰), and Italy (24.1 ‰, SD: 1.2 ‰). This gradient is consistent with climatic expectations, with higher δ^{18}O values in the warmer, more evaporative environment of Morocco (mean annual temperature; 16.7 °C; ~228 mm annual precipitation in the Taliouine region) and lower values in cooler, more humid regions such as Italy and Greece (Climate-Data.org, 2025). For comparison, Nie et al. (2023) reported Iranian saffron δ^{18}O values in close agreement with our Iranian results (25.2 ‰), suggesting that δ^{18}O for Iranian saffron remains relatively stable across seasons and years, likely reflecting consistent cultivation conditions in the main producing regions. In the same study, Chinese saffron showed a mean δ^{18}O of 24.9 ‰ (SD: 1.1 ‰), similar to values reported for Mediterranean growing regions such as Greece (24.8 ‰), where the saffron-producing region of Kozani is characterized by a mean annual temperature of ~12.4 °C and mean annual precipitation of ~568 mm (Hellenic National Meteorological Service, 2025). However, the Chinese samples originated from contrasting production areas, with humid eastern provinces and high-altitude Tibet (>4000 m) expected to yield more negative δ^{18}O values, while semi-arid central and southwestern regions would tend to have higher δ^{18}O values. This averaging effect results in a national mean that coincidentally aligns with Mediterranean levels (Nie et al., 2023). These findings highlight the importance of considering subnational variation when interpreting isotopic data, since δ^{18}O values are shaped by both regional climate conditions and cultivation environments. Consequently, δ^{18}O should be assessed at appropriate spatial scales rather than relying solely on national averages.

δ^{13}C values ranged from −30.2 ‰ in Morocco (mean: −26.0 ‰) to −22.8 ‰ in Iran (mean: −24.7 ‰). The relatively low mean δ^{13}C value for Italian saffron (−27.7 ‰) is consistent with C_3 plant metabolism under cooler, nutrient-rich conditions. By contrast, the higher δ^{13}C values observed in Iranian saffron likely reflect the combined effects of arid conditions and water stress, linked to reduce groundwater recharge during the growth period (Noori et al., 2023). In Mashhad, Iran's primary saffron-producing region, the rainless season extends for about

nine months (April to February), with August receiving on average only ~1 mm of precipitation. These dry conditions coincide with extreme summer heat, with peak daily temperatures in July reaching ~35 °C (WeatherSpark, 2025). These findings are broadly consistent with several previous studies. For instance, Maggi et al. (2011) reported nearly identical $\delta^{13}C$ values for Iranian saffron (mean: −24.5 ‰), which are further corroborated by Ghiasi & Parastar (2021) (mean: −24.6 ‰) and Nie et al. (2023) (mean: −25.0 ‰), highlighting the stability of carbon isotope signatures under Iran's prevailing agroclimatic conditions. For Italy, however, Maggi et al. (2011) reported slightly less negative $\delta^{13}C$ values (−26.6 ‰), most likely reflecting the warmer and drier conditions of their sampling locations. Rocchi et al. (2019) reported an intermediate mean $\delta^{13}C$ value of −26.6 ‰ for Italian saffron, but with a notably large standard deviation (±11.2 ‰), reflecting the diverse origins of their samples across both northern and central mainland regions (e.g., Abruzzo, Lombardy) as well as southern areas such as Sardinia. This wide variability underscores the influence of local agroclimatic conditions on carbon isotope ratios and reinforces the discriminatory power of $\delta^{13}C$ for tracing subregional origin.

$\delta^{15}N$ values ranged from 2.3 ‰ (Greece) to 5.8 ‰ (Morocco), with Moroccan saffron exhibiting the highest mean (5.8 ‰, SD: 3.5 ‰) and Greek samples the lowest (2.3 ‰, SD: 1.2 ‰). Higher $\delta^{15}N$ values in Moroccan saffron are consistent with the predominant use of organic fertilizers, particularly manure, which becomes enriched in ^{15}N through microbial mineralization and decomposition (Aziz & Sadok, 2015; Bateman et al., 2007; Vitòria et al., 2004). This practice aligns with Moroccan saffron cultivation soils characterized by coarse texture, low organic matter (<1 %), alkaline pH, and well-draining conditions typical of semi-arid zones, where manure addition is crucial to improve soil fertility and organic content (El Grah et al., 2022). In contrast, lower $\delta^{15}N$ values in Greek saffron align with Maggi et al. (2011), who reported even lower values (1.2 ‰, SD: 0.4 ‰), reflecting predominant use of synthetic nitrogen fertilizers or low-input systems relying mostly on natural nitrogen cycling. Greek saffron is typically cultivated in Mediterranean climates with hot, dry summers and mild, wet winters, characterized by average annual temperatures around 15 °C to 20 °C and annual precipitation of approximately 500 mm, mostly concentrated in spring, which is beneficial before flowering (Rocosaffron, 2025; Saffron Business, 2020). Such climatic conditions combined with well-drained soils reduce the need for organic amendments compared to Morocco. Spanish saffron exhibited intermediate $\delta^{15}N$ values (4.1 ‰, SD: 1.7 ‰), consistent with previous reports (Maggi et al., 2011), and similarly indicative of organic fertilizer use. Iranian saffron (3.7 ‰, SD: 1.1 ‰) closely matched literature values (Nie et al., 2023) and is consistent with the systematic application of synthetic nitrogen fertilizers in conjunction with clayey to sandy loam soils of low organic matter content (<1 %), typical of Iranian cultivation areas (Kafi et al., 2018; Mykhailenko et al., 2020). Italy displayed a wider $\delta^{15}N$ range, likely reflecting mixed fertilization practices, alternating between synthetic and organic inputs.

The sulfur isotopic composition of saffron primarily reflects the $\delta^{34}S$ signature of the soils and fertilizers used in cultivation. Regional geology strongly affects soil sulfur, as bedrock sulfates and sulfides vary widely in isotopic composition. Proximity to the coast can also play a role, since marine aerosols are typically enriched in ^{34}S compared with terrestrial sulfate. Agricultural practices contribute further variability: manure and organic fertilizers often show higher $\delta^{34}S$ values, while synthetic fertilizers tend to have lower $\delta^{34}S$ values. Biological fractionation in plants is generally small (−4 to +0.5 ‰ during assimilatory sulfate reduction), meaning that saffron largely records the isotopic composition of its sulfur source. Consequently, $\delta^{34}S$ values in saffron can serve as tracers of both regional geochemical background and cultivation practices. Morocco showed the highest country-level mean among regions with multiple samples (8.6 ‰, SD: 2.7 ‰), followed by Iran (7.6 ‰, SD: 4.4 ‰) and Italy (4.2 ‰, SD: 4.8 ‰), Spain (3.3 ‰), Slovenia (9.1 ‰), and the UK (6.0 ‰). Higher $\delta^{34}S$ in Moroccan saffron may reflect the combined influence of coastal marine sulfate deposition and/or manure-based fertilization and, while the lower values in Greece (3.8 ‰, SD: 1.2 ‰) are consistent with greater reliance on synthetic fertilizers. As noted by Perini et al. (2020), the isotopic composition of sulfur is influenced by multiple overlapping factors, making straightforward interpretation difficult despite its utility for origin discrimination. The lowest $\delta^{34}S$ value (−14.8 ‰) was observed in the Italian sample. Similar $\delta^{34}S$ value of −15.4 ‰ has been reported in truffles from Italy, suggesting that very low $\delta^{34}S$ is not a universal characteristic but rather a region-specific marker (Hamzić Gregorčič et al., 2020). In particular, such values are typical of the Perugia region, indicating a unique geochemical signature that may also be linked to saffron production in that region.

Significant regional differences were also identified in macroelements (Mg, K, Ca) and microelements (Mo, Sr, Fe), which can largely be attributed to variation in soil composition, fertilization, and irrigation practices. Magnesium concentrations ranged from 0.770 mg/g in Italian samples to 3.98 mg/g in Iranian saffron, with Iran showing the highest mean level (1.77 mg/g, SD: 0.55 mg/g). Potassium ranged from 5.57 mg/g (Italy) to 33.5 mg/g (Iran), with Spanish saffron exhibiting the highest mean concentration (19.9 mg/g, SD: 2.94 mg/g), followed closely by Iranian (18.7 mg/g, SD: 4.32 mg/g). Moroccan saffron displayed intermediate values (mean: 14.5 mg/g, SD: 2.18 mg/g), falling below Spanish and Iranian samples but above Italy.

These differences can be explained by agricultural practices and water management. In Italy, saffron is typically cultivated under rainfed conditions, with over 90 % of farms relying exclusively on local rainfall (Cicco et al., 2025; Giupponi et al., 2023). By contrast, saffron cultivation in Iran and Morocco involves controlled irrigation during key phenological stages, such as flowering (October) and the reproductive phase (March–April), often using groundwater or nutrient-rich water sources (Aziz & Sadok, 2015; Sepaskhah & Kamgar, 2009). Such practices directly influence mineral availability and uptake. The elevated K levels in Moroccan samples likely reflect the application of K-rich fertilizers, such as those supplied through the Khemisset Potash Project (Emmerson Plc, 2021). Similarly, Iran increased potash fertilizer use, including potassium sulfate (SOP) and Muriate of Potash (MOP), from the mid-1990s onward to improve yields (Malakouti, 2004). This trend is consistent with the observed antagonistic relationship between K^+ and Mg^{2+} in plant uptake, where increased K availability can suppress Mg absorption (Yang et al., 2024). The marked decrease in Mg concentrations in 2023 may therefore be linked to elevated potassium fertilization.

Industrial and agricultural activities also contribute to trace element patterns. Phosphate fertilizers are a recognized source of Cd and As in soils (Davenport & Peryea, 1991; Dharma-Wardana, 2018). In Greek saffron, elevated As levels may be linked to lignite mining in Western Macedonia, while vanadium enrichment in Iranian samples likely reflects oil extraction and related industrial activities (Vitòria et al., 2004). In arid regions, limited rainfall reduces leaching, leading to higher concentrations of soluble elements such as Rb in soils, which plants may then absorb more readily (Nathan, 2017).

Calcium and strontium concentrations also showed clear regional variation, reflecting underlying geology. Both elements are associated with carbonate-rich substrates, where limestone and dolomite enhance their availability through weathering (Boggs, 2006; Brand et al., 1998). Spanish saffron showed the highest mean Ca concentration (1.77 mg/g, SD: 0.803 mg/g), followed by Iranian (1.32 mg/g, SD: 0.77 mg/g). Italian samples exhibited the lowest mean Ca levels (0.287 mg/g, SD: 0.132 mg/g), while Moroccan saffron displayed intermediate values (0.883 mg/g, SD: 0.379 mg/g). Iranian saffron also had the highest Sr concentrations (mean: 11.3 μg/g, range: 1.64–28.0 μg/g), followed by Spanish (8.66 μg/g, range: 5.84–12.6 μg/g). Moroccan saffron contained the lowest mean Sr (2.12 μg/g), while Italian samples showed wide variability (0.358–59.1 μg/g; mean: 2.74 μg/g).

Other trace elements further underline environmental and agricultural influences. Italian saffron had the highest mean Mo concentration

(0.707 μg/g, SD: 0.436 μg/g), followed by Moroccan samples (0.574 μg/g, SD: 0.394 μg/g), while Greek (0.181 μg/g) and Spanish (0.304 μg/g) saffron showed lower levels. Iron concentrations varied markedly, from 30.3 μg/g in Italy to 2127 μg/g in Iran, with Iranian saffron showing the highest mean values (280 μg/g, SD: 341 μg/g). Aluminum also displayed strong regional contrasts, with Iranian samples ranging from 38.3 μg/g to 1758 μg/g (mean: 234 μg/g, SD: 297 μg/g), compared to consistently low values in Italy (mean: 31.0 μg/g, SD: 27.3 μg/g).

These findings align with earlier studies, such as those by D'Archivio et al. (2019), who highlighted elements like Sr, Ca, Mo, and Fe as key discriminants of saffron samples from Iran and Italy. The high variability of Fe and Al in our dataset further supports their role in distinguishing samples from diverse origins, particularly between saffron from Iran and Morocco. Ibourki et al. (2022) highlighted K as the dominant macroelement and Fe as the primary microelement in Moroccan agricultural products, reporting minimal variation in K concentrations across saffron samples. The results of the present study support this observation, as the standard deviation of K in Moroccan samples was 2.18 mg/g, indicating only moderate variability. The narrow range of K concentrations (10.2–18.9 mg/g) further supports the consistency of K levels, which likely reflects uniform soil conditions or agricultural practices in the sampled regions. This consistency with previous findings reinforces the geographical significance of these elements in agricultural products.

While the absolute concentrations of elements such as rubidium (Rb), strontium (Sr), potassium (K), and calcium (Ca) may change over time due to environmental or agricultural factors, their ratios (e.g., Rb/Sr, K/Rb, and Ca/Sr) provided more stable and reliable markers for geographical differentiation being less sensitive to temporal changes. The K/Rb ratio varies significantly across different rock and soil types, supporting its use in geographical separation. The Rb/Sr ratio helps trace environmental changes and geological events, such as volcanic activity, erosion, or sedimentation, which redistribute Rb and Sr in soils and rocks, leaving distinct geochemical markers (Nebel, 2014). Also, Ca/Sr has long been used as a chemical tracer in geochemistry and hydro-geochemistry (Land et al., 2000; Pett-Ridge et al., 2009), further validating its role in geographical differentiation. The variation in Rb/Sr, Ca/Sr, and K/Rb ratios between different countries provided valuable markers for regional differentiation (Fig. S3). Iranian saffron exhibits the highest and most variable K/Rb ratios, which are statistically significantly different from those of Italian and Moroccan samples. Italian saffron consistently shows higher Rb/Sr ratios, providing a strong marker to differentiate it from Iranian and Moroccan origins. The Ca/Sr ratio also proves effective for country-level separation despite fluctuations in absolute Ca and Sr concentrations. Moroccan saffron displays statistically significantly higher Ca/Sr values than Italian and Iranian samples, likely reflecting differences in carbonate content and weathering processes.

To further investigate the discriminatory potential of these variables, pairwise comparisons between the seven countries were conducted, focusing on the significantly different variables. These comparisons revealed distinct patterns in isotopic and elemental profiles that enabled differentiation between specific country pairs. The complete pairwise comparison results are provided in Table S5. For example, $\delta^{13}C$ and Sr clearly distinguished saffron from Greece and Iran, while $\delta^{2}H$, $\delta^{13}C$, and Mg were effective in differentiating saffron from Iran from Italy. Notably, Italian and Moroccan samples displayed significant differences across a broad range of elements, including $\delta^{2}H$, $\delta^{13}C$, $\delta^{15}N$, Mg, K, and Sr, among others. Samples from Slovenia and the United Kingdom ($n = 1$ each) showed no significant differences in pairwise comparisons, likely due to insufficient sample sizes and were excluded.

3.2. Orthogonal partial least squares discriminant analysis (OPLS-DA)

An OPLS-DA model was developed to differentiate saffron samples originating from Italy, Morocco, Iran, and Spain. The sufficient number of samples across the three studies provided a robust representation of geographical variation. For this differentiation, all stable isotopes were included alongside 18 elemental variables, as defined by the previously described criteria, supplemented with the Rb/Sr, K/Rb, and Ca/Sr ratios. Because the number of Spanish samples was limited, a separate OPLS-DA model was constructed to compare only Iranian and Spanish samples. This analysis achieved a clear separation between the two groups, with a classification accuracy of 97 %. The most discriminating variables were Ca/Sr, Rb, $\delta^{18}O$, Cd, Ca, and Co. For comparison, Wakefield et al. (2019) also reported a potential differentiation between Iranian and Spanish samples (from 2011) using LDA, where Ce, Al, Rb, Ba, and $\delta^{13}C$ were identified as key discriminators.

In the next step, we focused on three countries with comparable sample sizes. Because $\delta^{18}O$ and $\delta^{34}S$ were not measured in all cases, the analyses were performed using different parameter combinations. A summary of the results obtained from the various models is presented in Table 3. Models displayed moderate R^2X values (0.649–0.689), indicating that a substantial proportion of the systematic variability in the predictor data was modeled. At the same time, the models achieved high R^2Y values (0.733–0.810) and strong Q^2 values (0.698–0.771), which together confirm good model fit and predictive reliability. All OPLS-DA models were validated by permutation testing ($N = 200$) and CV-ANOVA. The permutation tests ($n = 200$) yielded R^2 intercepts ranging from 0.042 to 0.069 and Q^2 intercepts from −0.168 to −0.201 (Table 3).

These values are within accepted thresholds (R^2 intercept <0.3; Q^2 intercept <0), indicating that the models were not over fitted and that the observed discrimination is statistically significant. CV-ANOVA further confirmed model robustness, with highly significant p-values (< 0.0001) and large F values (> 38). Both models exhibited excellent classification performance, with Model M2 (incorporating Rb/Sr, K/Rb, and Ca/Sr ratios; Fig. 3) achieving 97 % overall accuracy. Notably, this model improved the correct classification of Moroccan samples from 92.4 % to 94.3 %. The inclusion of these ratios also underscored the distinctive isotopic and elemental signatures of Italian saffron, further supporting its clear separation from other regions. Among the most influential discriminators, Ca/Sr and K/Rb were particularly prominent.

Model M3, which incorporated $\delta^{18}O$ and $\delta^{34}S$ values alongside other isotopic parameters and without elemental ratios, achieved the highest classification accuracy (99 %), improving the correct classification rate for Moroccan samples to 98.1 %. The enhanced separation is primarily driven by $\delta^{18}O$, which clearly reflects water regime and climate: Moroccan saffron showed consistently higher $\delta^{18}O$ values (mean 27.6 ‰, SD 2.3 ‰) due to arid, evaporative conditions, compared with lower values in rain fed Italian saffron (mean 24.1 ‰, SD 1.2 ‰) and more stable values in irrigated Iranian saffron (mean 25.8 ‰, SD 1.2 ‰). In contrast, $\delta^{34}S$ contributed more modestly to the discrimination. Moroccan saffron tended toward higher $\delta^{34}S$ values (mean 8.6 ‰, SD 2.7 ‰), consistent with manure-based fertilization and possible marine sulfate deposition, while Iranian and Italian samples showed broader and partially overlapping ranges (means 7.6 ‰ and 4.2 ‰, respectively). Thus, $\delta^{34}S$ provides complementary but secondary information linked to nutrient sources and local geochemistry. Statistically significant differences were observed in $\delta^{18}O$ both between years and between regions, whereas $\delta^{34}S$ did not vary significantly between years but did show significant differences between countries (Table 2, Table S4). These orthogonal signals of water regime ($\delta^{18}O$) and nutrient source ($\delta^{34}S$) complement elemental markers such as K, Sr, and Ca, which may vary across years due to fertilizer application or drought. Their combined effect explains why the inclusion of $\delta^{18}O$ and $\delta^{34}S$ sharpened country-level boundaries in OPLS-DA, thereby reducing overlap and accounting for the higher classification accuracy achieved in Model M3.

3.3. Verifying labelling using class Modeling (DD-SIMCA)

Unlike discriminant methods, DD-SIMCA distinguishes objects of a particular class, i.e., the target class, from all other objects and classes,

Table 3
Summary of OPLS-DA models for discerning samples from Iran, Italy and Morocco.

Models based on	R^2X	R^2Y (cum)	Q^2 (cum)	Perm. R^2 int.	Perm. Q^2 int.	CV-ANOVA p	CV-ANOVA F	Parameters VIP > 1
M1: Stable isotopes and elemental analysis	0.661	0.733	0.698	0.042	−0.168	<0.0001	38.07	δ^2H, K, δ^{15}N, δ^{13}C, Mn, Ca, Sr, As
M2: Stable isotopes and elemental analysis with Rb/Sr, K/Rb, and Ca/Sr	0.689	0.801	0.760	0.060	−0.201	<0.0001	41.06	Ca/Sr, δ^2H, K, Sr, δ^{13}C, Mn, Ca, K/Rb, δ^{15}N, As
M3: Stable isotopes and elemental analysis with δ^{18}O and δ^{34}S	0.649	0.745	0.711	0.045	−0.184	<0.0001	41.88	δ^2H, δ^{18}O, K, δ^{13}C, Sr, Mn, Ca, As, δ^{15}N, Mg
M4: Stable isotopes and elemental analysis with δ^{18}O, δ^{34}S, Rb/Sr, K/Rb, and Ca/Sr	0.681	0.810	0.771	0.069	−0.198	<0.0001	44.18	Ca/Sr, δ^2H, K, Sr, δ^{18}O, δ^{13}C, K/Rb, Mn, Ca, δ^{15}N, As

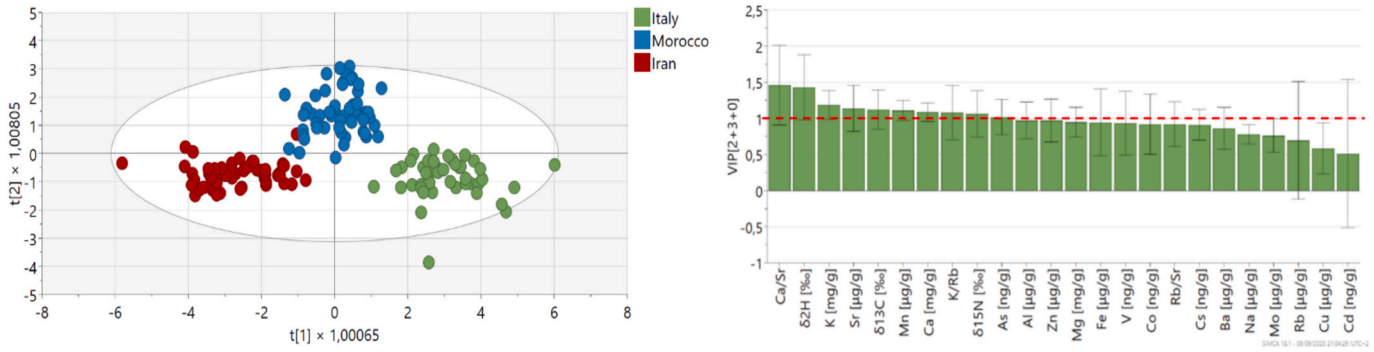

Fig. 3. OPLS-DA models differentiating geographical origins (Italy, Morocco, and Iran) based on isotopic ratios and elemental composition with Rb/Sr, K/Rb, and Ca/Sr excluding δ^{18}O and δ^{34}S values. Score plots (left) illustrate sample clustering by country: Italy (green), Morocco (purple), and Iran (red), with the 95 % confidence interval ellipse. Variable Importance in Projection (VIP) plots (right) highlight the most influential variables (VIP > 1, red dashed line) for group discrimination. (For interpretation of the references to color in this figure legend, the reader is referred to the web version of this article.)

referred to as alternative sets. The target sets were randomly divided into a training set (70 % of data from the primary dataset) and a test set (30 % of data from the primary dataset) to assess the model's validity. This value corresponds to a 4–5 fold cross-validation and represents a good compromise between having sufficient data to build a good model from the test dataset and the test dataset's error estimate (Gholamy et al., 2018). Also, the Procrustes cross-validation (Kucheryavskiy, Zhilin, Rodionova and Pomerantsev, 2020) was used for model optimization since it is a better alternative to regular cross-validation for short datasets. The exploratory data analysis was performed using the entire dataset with selected variables to explore the data structure and analyze the figure of merit (FoM) results concerning the number of PCs. A classification model was then built using the target set, the alternative set (samples from abroad) and the PCA model with a selected number of PCs. Sensitivity and specificity were used as figures of merit obtained from the target and alternative set.

Isotopic and elemental data, including δ^2H, δ^{13}C, δ^{15}N, and elemental concentrations such as Mg, Ca, Na, Fe, and several trace elements (e.g., Rb, Ba, Sr), were used to build the models for saffron samples originating from Italy, Morocco, and Iran. The selection of variables was optimized for each model. The three models showed excellent specificity (93.6–99.0 %) and sensitivity (94–99 %) across the data tested from Italian, Moroccan and Iranian samples (Table 4).

The model successfully identified whether saffron samples were of Italian origin. Two saffron samples fell outside the acceptance range for authentic Italian saffron and were thus classified as non-Italian (Fig. 4; 1A), which may reflect natural variability within Italian saffron. Further validation using authentic foreign samples from Iran, Morocco, Spain, Slovenia, and the United Kingdom confirmed the model's accuracy. However, one Moroccan sample was misclassified as Italian, suggesting an overlap in isotopic and elemental characteristics (Fig. 4; 1B).

This misclassification may stem from shared environmental factors, such as soil composition, climate, or agricultural practices. When verifying market samples labeled as originating from Spain, Italy, Iran, Greece, and Unknown sources, all were classified as non-Italian, including two samples explicitly labeled as Italian (Fig. 4; 1C) (Table S1). For Moroccan saffron classification, one authentic Moroccan saffron sample fell outside the acceptance range and was classified as non-Moroccan (Fig. 4; 2 A). Additionally, seven foreign saffron samples—two Italian, four Iranian, and one Greek—were misclassified as Moroccan (Fig. 4; 2B). Such finding suggests that saffron from these regions share chemical similarities with Moroccan saffron, making precise classification more challenging. When verifying market samples labeled as originating from Greece, Iran, Spain, Italy, and Unknown sources, all except three commercial Greek samples were correctly classified as non-Moroccan (Fig. 4; 2C). This raises concerns about potential misrepresentation in the saffron trade, where Moroccan saffron could be falsely marketed as Greek or vice versa, misleading consumers and undermining fair trade practices.

The model successfully identified the majority of authentic Iranian

Table 4
Summary of DD-SIMCA models used for distinguishing saffron samples according to the country of origin based on selected variables.

Country	Elements included	No. PC	TP	FN	TN	FP	Specificity (%)	Sensitivity (%)	TEFF (%)
Italy	δ^2H, δ^{13}C, δ^{15}N, Mg, K, Ca, Al, Mn, Fe, Cu, Zn, Rb, Ba, Sr, Mo, V, Co, Cd, As, Cs	4	38	2	117	1	99.0	95.0	97.0
Morocco	δ^2H, δ^{13}C, δ^{15}N, Mg, K, Al, Mn, Fe, Cu, Zn, Ba, Sr, Mo, V, Co, Cd, Cs	4	48	1	102	7	93.6	98.0	95.8
Iran	δ^2H, δ^{13}C, δ^{15}N, Mg, Ca, Na, Al, Mn, Fe, Rb, Ba, Sr, Mo, V, Co, Cd, As	4	46	1	104	6	94.5	97.9	96.0

PC – principal components; TP - a true positive; TN - a true negative; FP - a false positive; FN - a false negative; TEEF – total efficiency.

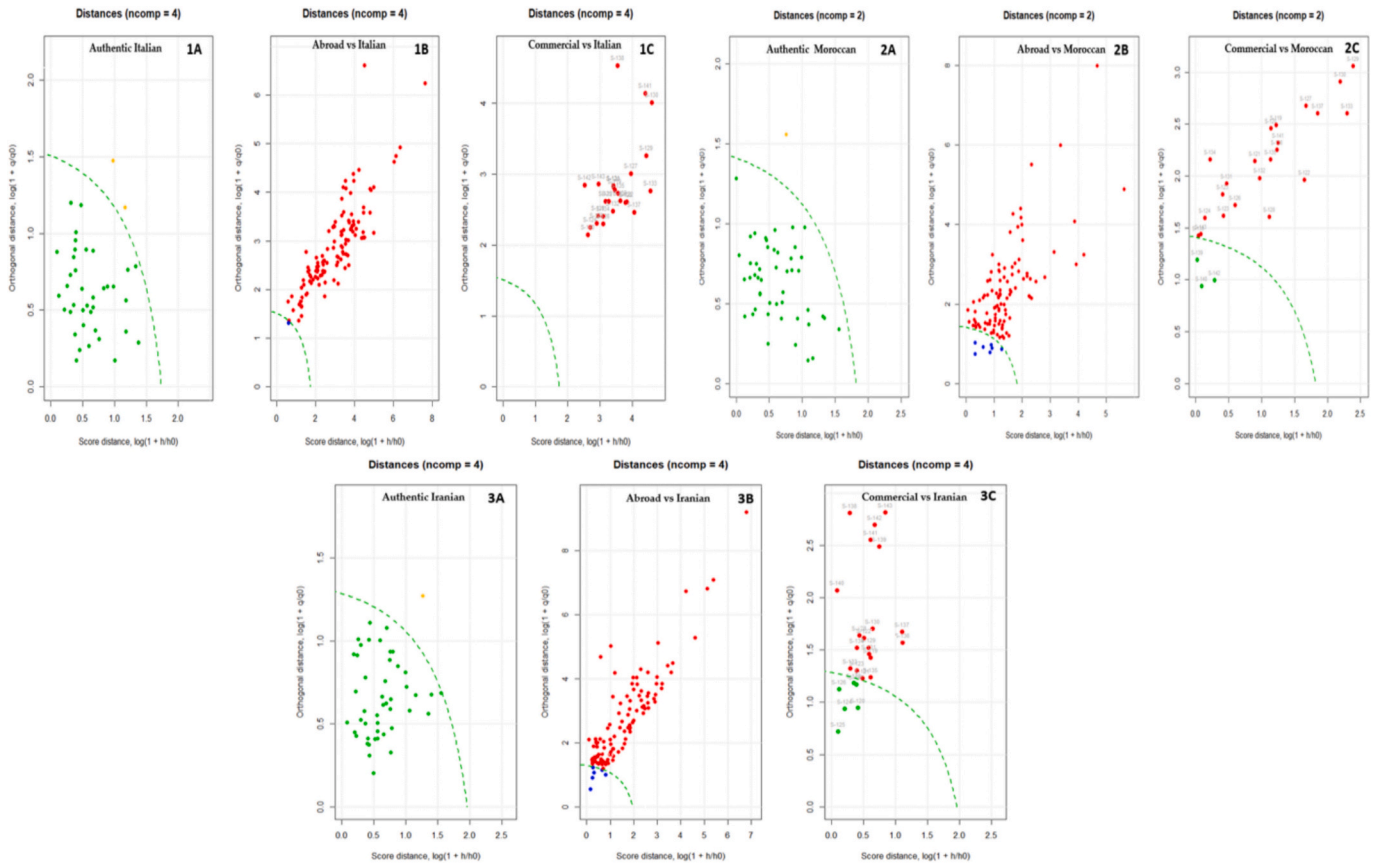

Fig. 4. DD-SIMCA classification model of a) authentic saffron samples (1 A, Italian, $n = 44$; 2 A, Moroccan, $n = 53$; 3 A, Iranian, $n = 52$), b) saffron samples cultivated outside the respective authentic regions (1B, Abroad vs Italian, $n = 118$; 2B, Abroad vs Moroccan, $n = 109$; 3B, Abroad vs Iranian, $n = 110$), c) commercial saffron samples (1C, Italian, $n = 25$; 2C, Moroccan, n = 25; 3C, Iranian, n = 25). The green dashed line represents the 100(1-α) % acceptance area, i.e., the decision boundary determining whether a sample belongs to the target class. Green points in a) indicate correctly identified authentic samples, while orange points represent wrongly rejected authentic samples based on the α value. Red points in b) denote true positive samples from abroad sources, while blue points indicate misclassified authentic samples. In c), red points represent commercial samples not falling within the authentic boundary, and green points represent misclassified commercial samples. (For interpretation of the references to color in this figure legend, the reader is referred to the web version of this article.)

saffron samples. However, one authentic Iranian sample was classified as non-Iranian (Fig. 4; 3 A). Additionally, six foreign samples—three Italian, two Moroccan, and one Spanish—were misclassified as Iranian (Fig. 4; 3B). When verifying market samples, all were classified as non-Iranian, except for six commercial Spanish samples and one unknown sample (Fig. 4; 3C). The misclassification of Spanish saffron as Iranian can be attributed to both natural isotopic and elemental similarities— as observed in previous results (Fig. 2), where authentic Iranian and Spanish samples exhibited significant overlap—and/or fraudulent mislabeling. This issue is particularly concerning given reports of large-scale saffron fraud in Spain, where Iranian saffron has been deliberately adulterated and sold as Spanish saffron to command higher prices (Europol, 2021). Interestingly, all six commercial samples labeled as Iranian fall outside the range of authentic samples, suggesting potential mislabeling.

3.3.1. *Quantitative assessment of misclassification*

To assess the extent of potential mislabeling, a total of 75 commercial saffron samples were evaluated using the classification model. The overall misclassification rate was calculated as:

$$\text{Misclassification Rate (\%)} = (\text{Total Misclassified Samples}/\text{Total Samples}) \times 100$$

Table 5
Potential mislabeling of commercial saffron samples by country of origin based on DD-SIMCA classification results.

Country	Total Samples	Misclassified	% Potential Mislabeling
Italy	25	2*	8 %
Morocco	25	3	12 %
Iran	25	6	24 %

* Two commercial samples explicitly labeled as Italian fell outside the authentic Italian range.

Among the analyzed samples, 11 were misclassified, corresponding to an overall misclassification rate of 14.7 % (~15 %). A country-specific breakdown (Table 5) revealed considerable variation, with the highest rate observed in samples labeled as Iranian (24 %). This finding is consistent with earlier reports of widespread saffron fraud, particularly involving the substitution or adulteration of Iranian saffron marketed as Spanish saffron to command higher market value.

These results highlight not only the robustness of the developed models in detecting inconsistencies but also the ongoing challenges in ensuring authenticity across the saffron supply chain. The observed misclassifications may reflect both natural overlaps in isotopic and elemental signatures between regions and deliberate mislabeling practices.

4. Conclusions

Saffron, one of the most valuable spices worldwide, is especially vulnerable to fraud and mislabeling, making authenticity verification essential for consumer trust and fair trade. This study demonstrates that stable isotope and multi-elemental analysis, integrated with advanced statistical modeling, offers a powerful and reliable tool for tracing saffron origin. By analyzing 163 authentic saffron samples-including 75 recently collected from Morocco, Greece, the United Kingdom, Slovenia, Spain, and Iran, together with two previously published datasets that were incorporated due to their strong methodological and analytical comparability-we achieved a robust classification accuracy of 94 %. Key isotopic and elemental markers (δ^2H, δ^{15}N, K, Ca, δ^{13}C, Sr, Mn, Co, and Zn), along with elemental ratios (Rb/Sr, K/Rb, Ca/Sr) and/or δ^{18}O and δ^{34}S, provided strong discriminatory power, enabling precise differentiation particularly for Moroccan saffron. The results further show that either elemental ratios or absolute elemental concentrations can be applied, depending on laboratory instrument availability. While δ^{18}O and δ^{34}S can sometimes be more challenging to obtain due to analytical constraints, their absence can be compensated by robust multi-elemental and other isotopic markers. Moreover, datasets from the literature can be integrated when analytical methods and stable isotope approaches are comparable, with stable isotope data generally offering greater robustness and consistency than elemental composition alone.

Application of DD-SIMCA further confirmed high specificity (95–98 %) and sensitivity (94–99 %) in authenticating saffron origins, while also revealing potential mislabeling in ~15 % of commercial samples. The highest misclassification rate was observed in products labeled as Iranian saffron (24 %), consistent with long-standing concerns about large-scale saffron fraud in this region. These findings reinforce the urgent need for robust authentication frameworks to safeguard traditional producers, enhance transparency in the saffron supply chain, and protect consumers from fraudulent practices.

Future work should focus on expanding global datasets and applying advanced statistical and artificial intelligence (AI) approaches to further improve predictive accuracy, scalability, and adaptability of saffron authenticity verification systems.

CRediT authorship contribution statement

Cathrine Terro: Writing – original draft, Project administration, Data curation, Conceptualization. **Lidija Strojnik:** Writing – review & editing, Visualization, Software, Data curation. **Doris Potočnik:** Methodology, Formal analysis. **Marta Jagodic Hudobivnik:** Validation, Data curation. **Darja Mazej:** Validation, Data curation. **Luana Bontempo:** Writing – review & editing, Resources, Formal analysis. **Mahmoud Eddabdouby:** Resources. **Nour Eddine Amenzou:** Resources. **Benmansour Moncef:** Resources. **Simon Kelly:** Resources, Project administration. **Nives Ogrinc:** Writing – review & editing, Supervision, Resources, Methodology, Funding acquisition, Conceptualization.

Declaration of competing interest

The authors declare that they have no known competing financial interests or personal relationships that could have appeared to influence the work reported in this paper.

Acknowledgements

Funding: We acknowledge the financial assistance of the FoodTraNet Project funded by the European Union's Horizon 2020 research and innovation programme under the MSCA Grant agreement No. 956265, PROMEDLIFE project (PRIMA programme supported by the European Union | Grant agreement No. 2132) and Slovenian Research and Innovation Agency by P1-0143. Samples were collected as a part of an IAEA funded CRP D52042: "Implementation of Nuclear Techniques for Authentication of Foods with High-Value Labelling Claims (INTACT Food)".

Appendix A. Supplementary data

Supplementary data to this article can be found online at https://doi.org/10.1016/j.fochx.2025.103196.

Data availability

Data will be made available on request.

References

Ayoub, I. B., Ara, S., & Lone, S. A. (2024). Evaluating the sensitivity of saffron yield to climate change in Western Himalaya, India: A study from Kashmir Valley. In *Climate crisis, social responses and sustainability: Socio-ecological study on global perspectives* (pp. 159–173). Springer Nature Switzerland. https://doi.org/10.1007/978-3-031-58261-5_7.

Aziz, L., & Sadok, W. (2015). Strategies used by the saffron producers of Taliouine (Morocco) to adapt to climate change. *Revue de géographie alpine, 103*(102). https://doi.org/10.4000/rga.2902

Bai, Y., Wang, X., Ha, L., Ao, Q., Dong, X., Guo, J., & Zhao, Y. (2025). Application of stable isotopes and mineral elements fingerprinting for beef traceability and authenticity in Inner Mongolia of China. *Food Chemistry, 465*, Article 141911. https://doi.org/10.1016/j.foodchem.2024.141911

Bateman, A. S., Kelly, S. D., & Woolfe, M. (2007). Nitrogen isotope composition of organically and conventionally grown crops. *Journal of Agricultural and Food Chemistry, 55*(7), 2664–2670. https://doi.org/10.1021/jf0627726

Bhooma, V., Nagasathiya, K., Vairamani, M., & Parani, M. (2020). Identification of synthetic dyes magenta III (new fuchsin) and rhodamine B as common adulterants in commercial saffron. *Food Chemistry, 309*, Article 125793. https://doi.org/10.1016/j.foodchem.2019.125793

Bhooma, V., Vassou, S. L., Kaliappan, I., & Parani, M. (2023). Identification of adulteration in the market samples of saffron using morphology, HPLC, HPTLC, and DNA barcoding methods. *Genome, 67*(2), 43–52. https://doi.org/10.1139/gen-2022-0059

Bizjak Bat, K., Eler, K., Mazej, D., Mozetič Vodopivec, B., Mulič, I., Kump, P., & Ogrinc, N. (2016). Isotopic and elemental characterization of Slovenian apple juice according to geographical origin: Preliminary results. *Food Chemistry, 203*, 86–94. https://doi.org/10.1016/j.foodchem.2016.02.039

Boggs, S. (2006). *Principles of sedimentology and stratigraphy* (vol. 662). Pearson Prentice Hall.

Bontempo, L., Camin, F., Ziller, L., Perini, M., Nicolini, G., & Larcher, R. (2017). Isotopic and elemental composition of selected types of Italian honey. *Measurement, 98*, 283–289. https://doi.org/10.1016/j.measurement.2015.11.022

Brand, U., Morrison, J. O., & Campbell, I. T. (1998). Strontium in sedimentary rocks. In *Geochemistry. Encyclopedia of Earth Science*. Dordrecht: Springer. https://doi.org/10.1007/1-4020-4496-8_301.

Brand, W. A., Coplen, T. B., Vogl, J., Rosner, M., & Prohaska, T. (2014). Assessment of international reference materials for isotope-ratio analysis (IUPAC Technical Report). *Pure and Applied Chemistry, 86*(3), 425–467. https://doi.org/10.1515/pac-2013-1023

Brunner, M., Katona, R., Stefánka, Z., & Prohaska, T. (2010). Determination of the geographical origin of processed spice using multielement and isotopic pattern on the example of Szegedi paprika. *European Food Research and Technology, 231*, 623–634. https://doi.org/10.1007/s00217-010-1314-7

Camin, F., Larcher, R., Perini, M., Bontempo, L., Bertoldi, D., Gagliano, G., … Versini, G. (2010). Characterization of authentic Italian extra-virgin olive oils by stable isotope ratios of C, O and H and mineral composition. *Food Chemistry, 118*(4), 901–909. https://doi.org/10.1016/j.foodchem.2008.04.059

Cardone, L., Castronuovo, D., Perniola, M., Cicco, N., & Candido, V. (2019). Evaluation of corm origin and climatic conditions on saffron (*Crocus sativus* L.) yield and quality. *Journal of the Science of Food and Agriculture, 99*, 5858–5869. https://doi.org/10.1002/jsfa.9860

Cardone, L., Castronuovo, D., Perniola, M., Scrano, L., Cicco, N., & Candido, V. (2020). The influence of soil physical and chemical properties on saffron (Crocus sativus L.) growth, yield and quality. *Agronomy, 10*, 1154. https://doi.org/10.3390/agronomy10081154

Cicco, N., Candido, V., Coluzzi, R., Imbrenda, V., Lanfredi, M., Larocca, M., … Sofo, A. (2025). Revitalizing marginal areas of Basilicata (Southern Italy) with saffron: A strategy approach mixing alternative cultivation system and land suitability analysis. *Land, 14*(4), 902. https://doi.org/10.3390/land14040902

Climate-Data.org. (2025). Climate data for cities worldwide. Retrieved September 28, 2025, from https://en.climate-data.org.

D'Archivio, A. A., Di Vacri, M. L., Ferrante, M., Maggi, M. A., Nisi, S., & Ruggieri, F. (2019). Geographical discrimination of saffron (*Crocus sativus* L.) using ICP-MS elemental data and class modeling of PDO Zafferano dell'Aquila produced in Abruzzo (Italy). *Food Analytical Methods, 12*, 2572–2581. https://doi.org/10.1007/s12161-019-01610-8

D'Archivio, A. A., Giannitto, A., Incani, A., & Nisi, S. (2014). Analysis of the mineral composition of Italian saffron by ICP-MS and classification of geographical origin. *Food Chemistry, 157*, 485–489. https://doi.org/10.1016/j.foodchem.2014.02.068

Davenport, J. R., & Peryea, F. J. (1991). Phosphate fertilizers influence leaching of lead and arsenic in a soil contaminated with lead arsenate. *Water, Air, and Soil Pollution, 57*, 101–110. https://doi.org/10.1007/BF00282873

Dharma-Wardana, M. W. C. (2018). Fertilizer usage and cadmium in soils, crops and food. *Environmental Geochemistry and Health, 40*(6), 2739–2759. https://doi.org/10.1007/s10653-018-0140-x

El Grah, F. Z., Bennasser, S. M., El Ghazali, H., Ait Hammou, R., Harrouni, C., & Daoud, S. (2022). Characterization of the Moroccan saffron in relation to climate, soil, and water in its main production zones. *Journal of Horticulture and Postharvest Research, 5*(2), 129–140. https://doi.org/10.22077/jhpr.2022.4487.1227

Emmerson Plc. (2021). Khemisset Potash Project. Retrieved December 2024, from https://www.emmersonplc.com/khemisset-potash-project.

Europol. (2021). A spice worth its weight in gold: Multi-million euros fake saffron trafficking scheme uncovered. Retrieved February 2025, from https://www.europol.europa.eu/media-press/newsroom/news/spice-worth-its-weight-in-gold-multi-million-euros-fake-saffron-trafficking-scheme-uncovered.

Fiamegos, Y., Dumitrascu, C., Papoci, S., & de la Calle, M. B. (2021). Authentication of PDO paprika powder (Pimentón de la Vera) by multivariate analysis of the elemental fingerprint determined by ED-XRF. A feasibility study. *Food Control, 120*, Article 107496. https://doi.org/10.1016/j.foodcont.2020.107496

Fidelis, M., Santos, J. S., Coelho, A. L. K., Rodionova, O. Y., Pomerantsev, A., & Granato, D. (2017). Authentication of juices from antioxidant and chemical perspectives: A feasibility quality control study using chemometrics. *Food Control, 73*, 796–805. https://doi.org/10.1016/j.foodcont.2016.09.043

Forina, M., Oliveri, P., Lanteri, S., & Casale, M. (2008). Class-modeling techniques, classic and new, for old and new problems. *Chemometrics and Intelligent Laboratory Systems, 93*(2), 132–148. https://doi.org/10.1016/j.chemolab.2008.05.003

Ghiasi, S., & Parastar, H. (2021). Chemometrics-assisted isotope ratio fingerprinting based on gas chromatography/combustion/isotope ratio mass spectrometry for saffron authentication. *Journal of Chromatography A, 1657*, 462587. https://doi.org/10.1016/j.chroma.2021.462587

Gholamy, A., Kreinovich, V., & Kosheleva, O. (2018). Why 70/30 or 80/20 relation between training and testing sets: A pedagogical explanation. *Departmental Technical Reports (CS), 1209*. Retrieved from https://scholarworks.utep.edu/cs_techrep/1209.

Giannioti, Z., Brigante, F. I., Kelly, S., Ogrinc, N., Hudobivnik, M. J., Mazej, D., … Bontempo, L. (2024). Authentication of premium Asian rice varieties: Stable isotope ratios and multi-elemental content for the identification of geographic fingerprints. *LWT, 209*, Article 116752. https://doi.org/10.1016/j.lwt.2024.116752

Giupponi, L., Leoni, V., Sala, S., Giorgi, A., & Bertoni, D. (2023). Saffron growing in Italy: A sustainable secondary activity for farms in hilly and sub-mountain areas. *International Journal of Agricultural Sustainability, 21*(1), Article 2270263. https://doi.org/10.1080/14735903.2023.2270263

Gresta, F., Lombardo, G. M., Siracusa, L., & Ruberto, G. (2009). Saffron, an alternative crop for sustainable agricultural systems: A review. In *Sustainable Agriculture* (pp. 355–376). https://doi.org/10.1007/978-90-481-2666-8_23

Hamzić Gregorčič, S., Strojnik, L., Potočnik, D., Vogel-Mikuš, K., Jagodic, M., Camin, F., … Ogrinc, N. (2020). Can we discover truffle's true identity? *Molecules, 25*(9), 2217. https://doi.org/10.3390/molecules25092217

Hellenic National Meteorological Service. (2025). *Climatology data for Kozani, West Macedonia region*. Hellenic National Meteorological Service. Retrieved September 30, 2025, from http://oldportal.emy.gr/emy/en/climatology/climatology_city?periferia=West%20Macedonia&poli=Kozani.

Hiraoka, H., Morita, S., Izawa, A., Aoyama, K., Shin, K. C., & Nakano, T. (2016). Tracing the geographical origin of onions by strontium isotope ratio and strontium content. *Analytical Sciences, 32*(7), 781–788. https://doi.org/10.2116/analsci.32.781

Ibourki, M., Gharby, S., El Hani, O., Digua, K., Amine, A., Ahmed, M. N., … El Hammadi, A. (2022). Elemental profiling and geographical differentiation of saffron (Crocus sativus L.) using inductively coupled plasma-optical emission spectroscopy (ICP-OES) and principal component analysis. *Chemical Data Collections, 41*, Article 100937. https://doi.org/10.1016/j.cdc.2022.100937

ISPRA. (2020). *Temperature and precipitation 1991–2020 climatic normals over Italy*. Rome: Istituto Superiore per la Protezione e la Ricerca Ambientale. https://www.isprambiente.gov.it.

Kafi, M., Kamili, A. N., Husaini, A. M., Ozturk, M., & Altay, V. (2018). An expensive spice saffron (Crocus sativus L.): A case study from Kashmir, Iran, and Turkey. In M. Ozturk, M. Hakeem, & A. M. Ashraf (Eds.), *Global perspectives on underutilized crops* (pp. 109–149). Springer. https://doi.org/10.1007/978-3-319-77776-4_4.

Katerinopoulou, K., Kontogeorgos, A., Salmas, C. E., Patakas, A., & Ladavos, A. (2020). Geographical origin authentication of Agri-food products: A review. *Foods, 9*(4), 489. https://doi.org/10.3390/foods9040489

Kelly, S., Heaton, K., & Hoogewerff, J. (2005). Tracing the geographical origin of food: The application of multi-element and multi-isotope analysis. *Trends in Food Science & Technology, 16*, 555–567.

Koocheki, A., & Milani, E. (2020). Saffron adulteration. In *Saffron* (pp. 321–334). Woodhead Publishing.

Kucheryavskiy, S. (2020). mdatools—R package for chemometrics. *Chemometrics and Intelligent Laboratory Systems, 198*, Article 103937. https://doi.org/10.1016/j.chemolab.2020.103937

Kucheryavskiy, S., Zhilin, S., Rodionova, O., & Pomerantsev, A. (2020). Procrustes cross-validation—a bridge between cross-validation and independent validation sets. *Analytical Chemistry, 92*(17), 11842–11850. https://doi.org/10.1021/acs.analchem.0c02175

Land, M., Ingri, J., Andersson, P. S., & Öhlander, B. (2000). Ba/Sr, ca/Sr and $^{87}Sr/^{86}Sr$ ratios in soil water and groundwater: Implications for relative contributions to stream water discharge. *Applied Geochemistry, 15*(3), 311–325. https://doi.org/10.1016/S0883-2927(99)00054-2

Liu, H., Qin, Y., Ma, Q., Zhao, Q., Guo, X., Ma, L., & Zhang, J. (2021). Discrimination of the geographical origin of Yanchi tan lamb with different muscle sections by stable isotopic ratios and elemental profiles. *International Journal of Food Science & Technology, 56*(6), 2604–2611. https://doi.org/10.1111/ijfs.14900

Luo, R., Jiang, T., Chen, X., Zheng, C., Liu, H., & Yang, J. (2019). Determination of geographic origin of Chinese mitten crab (Eriocheir sinensis) using integrated stable isotope and multi-element analyses. *Food Chemistry, 274*, 1–7. https://doi.org/10.1016/j.foodchem.2018.08.104

Maggi, L., Carmona, M., Kelly, S. D., Marigheto, N., & Alonso, G. L. (2011). Geographical origin differentiation of saffron spice (*Crocus sativus* L. stigmas)—preliminary investigation using chemical and multi-element (H, C, N) stable isotope analysis. *Food Chemistry, 128*(2), 543–548. https://doi.org/10.1016/j.foodchem.2011.03.063

Mahynski, N. A., Strojnik, L., Shen, V. K., & Ogrinc, N. (2025). Comparing machine learning models to chemometric ones to detect food fraud: A case study in Slovenian fruits and vegetables. *Food Chemistry*. , Article 144569. https://doi.org/10.1016/j.foodchem.2025.144569

Malakouti, M. J. (2004, November). The Iranian experiences in fertigation and use of potash fertilizers. In *IPI regional workshop on potassium and fertigation development in West Asia and North Africa; Rabat, Morocco*.

Menia, M., Iqbal, S., Zahida, R., Tahir, S., Kanth, R. H., Saad, A. A., & Hussian, A. (2018). Production technology of saffron for enhancing productivity. *Journal of Pharmacognosy and Phytochemistry, 7*(1), 1033–1039.

Moras, B., Pouchieu, C., Gaudout, D., Rey, S., Anchisi, A., Saupin, X., & Jame, P. (2022). Authentication of Iranian saffron (Crocus sativus) using stable isotopes $\delta^{13}C$ and $\delta^{2}H$ andmetabolites quantification. *Molecules, 27*, 6801. https://doi.org/10.3390/molecules27206801

Mousavi, S. Z., & Bathaie, S. Z. (2011). Historical uses of saffron: Identifying potential new avenues for modern research. *Avicenna Journal of Phytomedicine, 1*(2), 57.

Mykhailenko, O., Desenko, V., Ivanauskas, L., & Georgiyants, V. (2020). Standard operating procedure of Ukrainian saffron cultivation according to good agricultural and collection practices to assure quality and traceability. *Industrial Crops and Products, 151*, Article 112376. https://doi.org/10.1016/j.indcrop.2020.112376

Mzabri, I., Addi, M., & Berrichi, A. (2019). Traditional and modern uses of saffron (Crocus sativus). *Cosmetics, 6*(4), 63. https://doi.org/10.3390/cosmetics6040063

Nathan, M. V. (2017). Soils, plant nutrition and nutrient management (revised January 2017, chapter 4). In *Soil Testing and Plant Diagnostic Service Laboratory*. University of Missouri Extension.

Nebel, O. (2014). Rb–Sr dating. In W. Rink, & J. Thompson (Eds.), *Encyclopedia of scientific dating methods*. Dordrecht: Springer. https://doi.org/10.1007/978-94-007-6326-5_116-1.

Ni, X., Li, X., Ran, G., Chen, J., Jiang, X., Sun, J., & Bai, W. (2022). Determination of the geographical origin of Trachinotus ovatus and Pampus argenteus in China by multi-element and stable isotope analysis. *Food Chemistry, 394*, Article 133457. https://doi.org/10.1016/j.foodchem.2022.133457

Nie, J., Yang, J., Liu, C., Li, C., Shao, S., Yao, C., … Yuan, Y. (2023). Stable isotope and elemental profiles determine geographical origin of saffron from China and Iran. *Food Chemistry, 405*, Article 134733. https://doi.org/10.1016/j.foodchem.2022.134733

Noori, R., Maghrebi, M., Jessen, S., Bateni, S. M., Heggy, E., Javadi, S., … AghaKouchak, A. (2023). Decline in Iran's groundwater recharge. *Nature Communications, 14*(1), 6674. https://doi.org/10.1038/s41467-023-42411-2

Opatić, A. M., Nečemer, M., Kocman, D., & Lojen, S. (2017). Geographical origin characterization of Slovenian organic garlic using stable isotope and elemental composition analyses. *Acta Chimica Slovenica, 64*(4). https://doi.org/10.17344/acsi.2017.3476

Perini, M., Pianezze, S., Ziller, L., Ferrante, M., Ferella, F., Nisi, S., … D'Archivio, A. A. (2020). Stable isotope ratio analysis combined with inductively coupled plasma-mass spectrometry for geographical discrimination between Italian and foreign saffron. *Journal of Mass Spectrometry, 55*(11), Article e4595. https://doi.org/10.1002/jms.4595

Pett-Ridge, J. C., Derry, L. A., & Barrows, J. K. (2009). Ca/Sr and $^{87}Sr/^{86}Sr$ ratios as tracers of ca and Sr cycling in the Rio Icacos watershed, Luquillo Mountains, Puerto Rico. *Chemical Geology, 267*(1–2), 32–45. https://doi.org/10.1016/j.chemgeo.2008.11.022

Potočnik, D., Jagodic Hudobivnik, M., Mazej, D., & Ogrinc, N. (2021). Optimization of the sample preparation method for determination of multi-elemental composition in fruit samples by ICP-MS analysis. *Measurement: Sensors, 18*, Article 100292. https://doi.org/10.1016/j.measen.2021.100292

Primožič, S., Terro, C., Strojnik, L., Šegatin, N., Poklar Ulrih, N., & Ogrinc, N. (2025). Assessing the authenticity and quality of paprika (Capsicum annuum) and cinnamon

(Cinnamomum spp.) in the Slovenian market: A multi-analytical and chemometric approach. *Foods, 14*(13), 2323. https://doi.org/10.3390/foods14132323
Rahimi, H., Shokrpour, M., Tabrizi Raeini, L., & Esfandiari, E. (2017). A study on the effects of environmental factors on vegetative characteristics and corm yield of saffron (Crocus sativus). *Iranian Journal of Horticultural Science, 48*, 45–52. https://doi.org/10.22059/ijhs.2017.224869.1165
Rikabad, M. M., Pourakbar, L., Moghaddam, S. S., & Popović-Djordjević, J. (2019). Agrobiological, chemical and antioxidant properties of saffron (Crocus sativus L.) exposed to TiO_2 nanoparticles and ultraviolet-B stress. *Industrial Crops and Products, 137*, 137–143. https://doi.org/10.1016/j.indcrop.2019.05.017
Rocchi, R., Mascini, M., Faberi, A., Sergi, M., Compagnone, D., Di Martino, V., … Pittia, P. (2019). Comparison of IRMS, GC-MS, and E-nose data for the discrimination of saffron samples with different origin, process, and age. *Food Control, 106*, Article 106736. https://doi.org/10.1016/j.foodcont.2019.106736
Rocosaffron. (2025). Saffron growing temperature guide. https://www.rocosaffron.com/blogs/saffron-hub/saffron-growing-temperature-guide.
Rodionova, O. Y., Oliveri, P., & Pomerantsev, A. L. (2016). Rigorous and compliant approaches to one-class classification. *Chemometrics and Intelligent Laboratory Systems, 159*, 89–96. https://doi.org/10.1016/j.chemolab.2016.10.002
Rodionova, O. Y., Titova, A. V., & Pomerantsev, A. L. (2016). Discriminant analysis is an inappropriate method of authentication. *Trends in Analytical Chemistry, 78*, 17–22. https://doi.org/10.1016/j.trac.2016.01.010
Ryparova Kvirencova, J., Navratilova, K., Hrbek, V., & Hajslova, J. (2023). Detection of botanical adulterants in saffron powder. *Analytical and Bioanalytical Chemistry, 415*(23), 5723–5734. https://doi.org/10.1007/s00216-023-04853-x
Saaltink, R., Griffioen, J., Mol, G., & Birke, M. (2014). Geogenic and agricultural controls on the geochemical composition of European agricultural soils. *Journal of Soils and Sediments, 14*(1), 121–137.
Saffron Business. (2020). Saffron cultivation. https://www.saffronbusiness.com/saffron-cultivation/.
Salehi, A., Shariatifar, N., Pirhadi, M., & Zeinali, T. (2022). An overview on different detection methods of saffron (*Crocus sativus* L.) adulterants. *Journal of Food Measurement and Characterization, 16*(6), 4996–5006. https://doi.org/10.1007/s11694-022-01586-w
Sepaskhah, A. R., & Kamgar, H. A. A. (2009). Saffron irrigation regime. Retrieved from https://www.sid.ir/en/Journal/ViewPaper.aspx?ID=175240.
Shahi, T., Assadpour, E., & Jafari, S. M. (2016). Main chemical compounds and pharmacological activities of stigmas and tepals of 'red gold' saffron. *Trends in Food Science & Technology, 58*, 69–78. https://doi.org/10.1016/j.tifs.2016.10.010
Siracusa, L., Gresta, F., Avola, G., Lombardo, G. M., & Ruberto, G. (2010). Influence of corm provenance and environmental condition on yield and apocarotenoid profiles in saffron (*Crocus sativus* L.). *Journal of Food Composition and Analysis, 23*, 394–400. https://doi.org/10.1016/j.jfca.2010.02.007
Skordas, K., Papastergios, G., & Filippidis, A. (2013). Major and trace element contents in apples from a cultivated area of Central Greece. *Environmental Monitoring and Assessment, 185*(10), 8465–8471.
Smith, R. G. (2005). Determination of the country of origin of garlic (*Allium sativum*) using trace metal profiling. *Journal of Agricultural and Food Chemistry, 53*(10), 4041–4045.
Starling, M. (2023). *Morocco rolls out a phosphorous-fueled plan to heal soils across Africa*. Mongabay. https://news.mongabay.com/2023/07/morocco-rolls-out-a-phosphorous-fueled-plan-to-heal-soils-across-africa/.
Strojnik, L., Potočnik, D., Jagodic Hudobivnik, M., Mazej, D., Japelj, B., Škrk, N., Marolt, S., Heath, D., & Ogrinc, N. (2022). Geographical identification of strawberries based on stable isotope ratio and multi-elemental analysis coupled with multivariate statistical analysis: A Slovenian case study. *Food Chemistry, 381*, Article 132204. https://doi.org/10.1016/j.foodchem.2022.134733
Terro, C., Modic, R., Ogrinc, M., Simčič, A., Drole, J., Eftimov, T., … Ogrinc, N. (2025). IsoFoodTrack: A comprehensive database and management system based on stable isotope ratio analysis for combating food fraud. *Frontiers in Nutrition, 12*, Article 1516521. https://doi.org/10.3389/fnut.2025.1516521
Toreti, A., Bavera, D., Acosta Navarro, J., et al. (2023). *Drought in the Maghreb and Türkiye February 2023*. Luxembourg: Publications Office of the European Union. https://doi.org/10.2760/24467. JRC132915.
Vitòria, L., Otero, N., Soler, A., & Canals, À. (2004). Fertilizer characterization: Isotopic data (N, S, O, C, and Sr). *Environmental Science & Technology, 38*(12), 3254–3262. https://doi.org/10.1021/es0348187
Wakefield, J., McComb, K., Ehtesham, E., Van Hale, R., Barr, D., Hoogewerff, J., & Frew, R. (2019). Chemical profiling of saffron for authentication of origin. *Food Control, 106*, Article 106699. https://doi.org/10.1016/j.foodcont.2019.06.025
WeatherSpark. (2025). Average weather data. Retrieved September 28, 2025, from https://weatherspark.com/.
Wu, Z., Chen, L., Wu, L., Xue, X., Zhao, J., Li, Y., … Lin, G. (2015). Classification of Chinese honeys according to their floral origins using elemental and stable isotopic compositions. *Journal of Agricultural and Food Chemistry, 63*(22), 5388–5394. https://doi.org/10.1021/acs.jafc.5b01576
Yang, M., Zhou, D., Hang, H., Chen, S., Liu, H., Su, J., Lv, H., Jia, H., & Zhao, G. (2024). Effects of balancing exchangeable cations Ca, Mg, and K on the growth of tomato seedlings (*Solanum lycopersicum* L.) based on increased soil cation exchange capacity. *Agronomy, 14*(3), 629. https://doi.org/10.3390/agronomy14030629
Zarghani, F., Karimi, A., Khorasani, R., & Lakzian, A. (2016). To evaluate the effect of soil physical and chemical characteristics on the growth characteristics of saffron (*Crocus sativus* L.) corms in Tornbat-e Heydariyeh area. *Journal of Agroecology, 8*, 120–133. https://doi.org/10.22067/jag.v8i1.48511
Zhang, T., Li, S., Wang, Y., Hu, Q., Wang, C., Yang, H., & Xu, N. (2022). Research progress in the application of stable isotope and mineral element analysis in tracing the geographical origin of Chinese medicinal materials. *Food Science and Technology, 42*, Article e08222. https://doi.org/10.1590/fst.08222
Zhao, S., Qiu, C., Zhang, T., Hu, X., Zhao, Y., Cheng, X., & Chen, C. (2022). Effects of fertilizer on the quality and traceability of Tibet highland barley (Hordeum vulgare L.): A diagnosis using nutrients and mineral elements. *Foods, 11*(21), 3397. https://doi.org/10.3390/foods11213397
Zontov, Y. V., Rodionova, O. Y., Kucheryavskiy, S. V., & Pomerantsev, A. L. (2017). DD-SIMCA–a MATLAB GUI tool for data driven SIMCA approach. *Chemometrics and Intelligent Laboratory Systems, 167*, 23–28. https://doi.org/10.1016/j.chemolab.2017.05.010